

04.1

## Influence of discharge chamber parameters on the efficiency of ozone generation by pulsed corona discharge

© I.E. Filatov, Yu.S. Surkov, D.L. Kuznetsov

Institute of Electrophysics, Ural Branch, Russian Academy of Sciences, Yekaterinburg, Russia  
E-mail: fil@iep.uran.ru

Received April 1, 2022

Revised April 21, 2022

Accepted May 13, 2022

The article discusses ways to increase the efficiency of ozone production in a coaxial chamber using a pulsed corona discharge. The effect of the discharge gap and the diameter of the potential electrode on the energy efficiency of ozone production using a pulsed corona discharge of negative polarity with duration of 40 ns and voltage of about 100 kV was investigated. It is shown that with an increase in the discharge gap, the productivity of the installation decreases, and the energy efficiency increases. The optimal diameter of the potential electrode has a value of about 0.64 mm. This information will be useful in the development of highly efficient ozonators and in optimizing the parameters of plasma–chemical reactors for air purification by electro–discharge methods.

**Keywords:** pulsed corona discharge, ozone, non–equilibrium plasma, ozonator.

DOI: 10.21883/TPL.2022.07.54032.19210

The ozone synthesis is one of the best–studied commercial plasma–chemical processes. However, the problem of the energy efficiency of ozone production remains topical, which continuously stimulates investigations devoted to optimizing the electrical–discharge method for ozone production. High energy efficiency is characteristic of setups involving a barrier discharge that allows obtaining the ozone specific output of up to  $538 \text{ g} \cdot \text{kW} \cdot \text{h}^{-1}$  [1]. Comparative analysis of modifications of the barrier and corona discharges was performed in reviews [2–5]. Issues concerning the ozonator parameters with respect to the flow rate and pulse parameters have been considered in [6]. A review of various methods for producing ozone in combination with chemically interacting components is presented in [7]. Comparison of different–type discharges and their parameters exhibits perspectiveness of using nanosecond pulsed discharges [8,9]. An important advantage of such generators consists also in lower requirements for insulation inside the discharge chamber of a plasma–chemical reactor (PCR). The role of ozone and its conversion with formation of chemically active plasma has been considered in [10]. A major part of investigations deals with ozonators of the coaxial wire–cylinder design [9,11,12].

Designs of ozonators and plasma–chemical setups for cleaning air from volatile organic compounds are, in most cases, identical. For assessing the PCR plasma–chemical efficiency with respect to impurity removal, it is proposed to use its ozone production efficiency [13]. The process of plasma–chemical treatment of oxygen–containing gas mixtures is always accompanied by generation of ozone whose reaction ability is insufficient for fast binding of impurities; therefore, the ozone generation should be

always taken into account because of its high toxicity and in view of further utilizing its oxidation potential in catalytic systems [14–16]. An efficient way of supplying power to PCR and ozonators is to use pulse generators that form high–voltage nanosecond pulses based on the semiconductor opening switch effect (SOS–effect) [12,17].

The wire–cylinder design of the PCR coaxial chamber is minimally affected by contamination with products of volatile impurities resinification. Though there is a great variety of methods employing such a design, the influence of PCR dimensional parameters are studied rarely. For instance, despite the nanosecond discharge

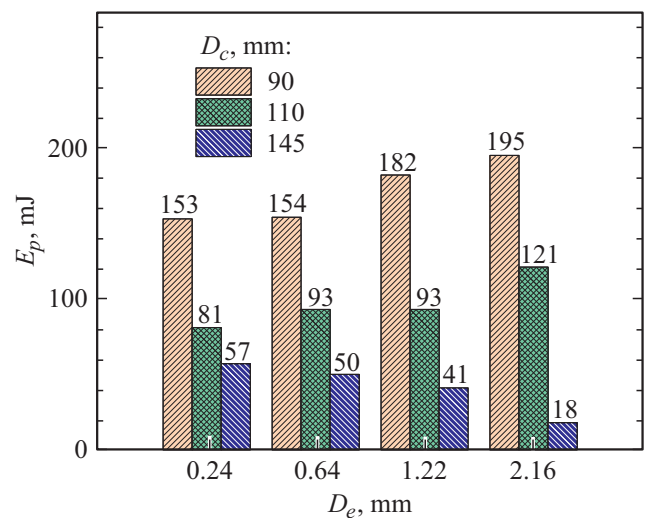


**Figure 1.** Mean pulse energy  $E_p$  versus the discharge gap parameters: potential electrode diameter  $D_e$  and outer cylinder diameter  $D_c$ .

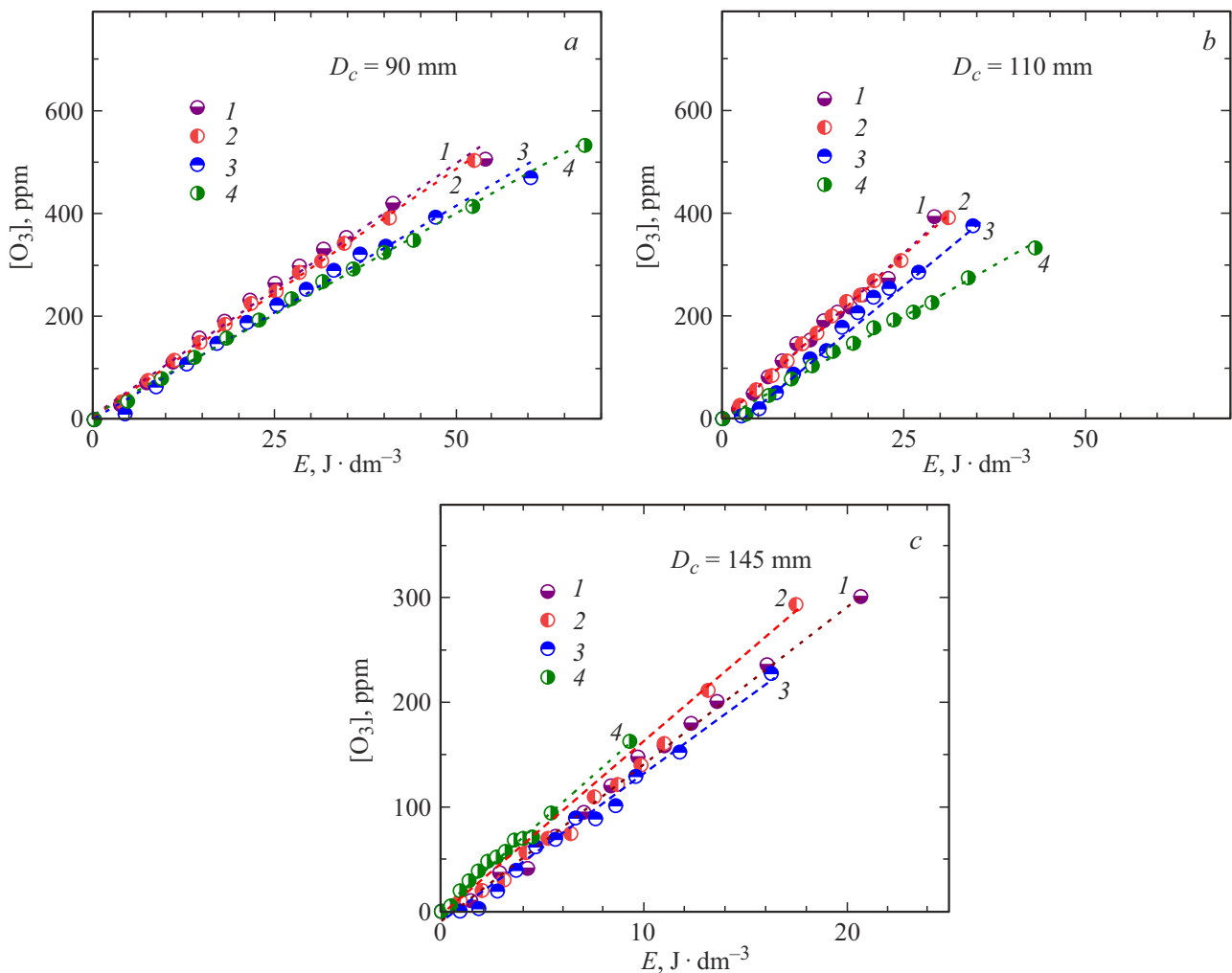


**Figure 2.** Ozone concentration  $[O_3]$  versus specific energy  $E$  for the inner electrode diameters  $D_e = 0.24$  (1),  $0.64$  (2),  $1.22$  (3),  $2.16$  mm (4) at the external cylindrical electrode diameters  $D_c = 90$  (a),  $110$  (b) and  $145$  mm (c).

efficiency with respect to the ozone generation is proved experimentally, the influence of such discharge system parameters as „potential electrode diameter–outer cylinder diameter“ on the ozone generation efficiency has not been systematically investigated almost at all. Such an investigation is considered in this paper. This information will be useful not only for developing highly efficient ozonators but also for adjusting parameters of the PCR discharge chamber for removing harmful impurities from air releases.

The experimental setup design described in details in [18] is of the modular type and enables easy variation of the discharge gap parameters. The PCR setup gas mixture is efficiently agitated in the closed–cycle mode in order to quickly equalize concentrations of all the components, which allows improvement of the analysis results reproducibility. The high–voltage pulse generator was constructed based on a circuit involving SOS–switches [17]. The discharge parameters were as follows: negative–polarity voltage 100 kV in magnitude, current 60–150 A in mag-

nitude, bell–shaped pulse length at half maximum of 40 ns, pulse repetition rate of  $f = 10$  Hz. The discharge system of the plasma–chemical reactor consisted of a stainless–steel cylinder 560 mm long with three inner diameters  $D_c = 90$ , 110 and 145 mm. Along the cylinder axis a potential electrode was stretched, which was made from guitar strings of four diameters  $D_e = 0.24$ ,  $0.64$ ,  $1.22$  and  $2.16$  mm. Air was simulated by a commercial gas mixture „Synthetic air“ with the composition ratio  $N_2 : O_2 = 80 : 20$  (by volume). The experiments were performed at room temperature, the pressure in the chamber was set to the ambient (atmospheric) pressure and remained equal to 94–98 kPa during all the experiments. It is worth noticing that all the experiments were performed under comparable conditions. The chamber’s internal volume was preliminary evacuated and blown–through twice with the operating gas mixture. The ozone concentration was measured every minute during first ten minutes of the gas mixture treatment; after that, the concentration was measured in extra 2 and 4 min of treatment. This algorithm was used in order to reveal the linear

Ozone specific output  $G_{O_3}$  versus the electrode system parameters

Cylinder inner diameter $D_c$ , mm	$G_{O_3}$ , g · kW · h <sup>-1</sup>			
	$D_e = 0.24$ mm	$D_e = 0.64$ mm	$D_e = 1.22$ mm	$D_e = 2.16$ mm
90	75 ± 2	74 ± 1	63 ± 2	60 ± 1
110	100 ± 3	97 ± 2	89 ± 3	61 ± 2
145	115 ± 3	131 ± 6	111 ± 4	132 ± 4

Note.  $D_e$  is the potential electrode diameter.

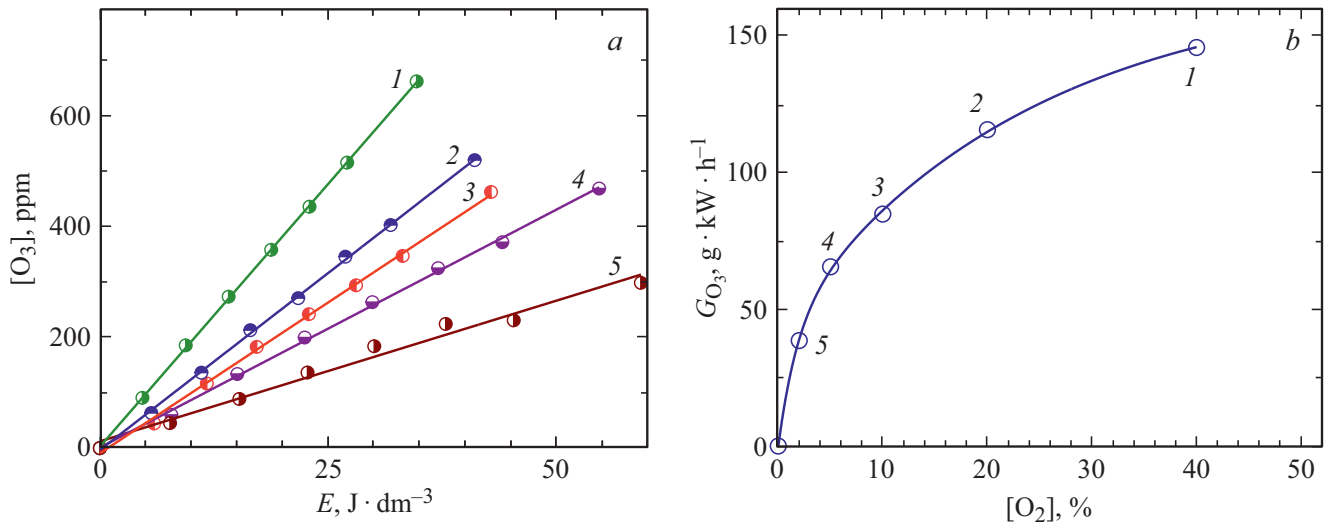


**Figure 3.** *a* — ozone concentration  $[O_3]$  versus specific energy  $E$  in the nitrogen–oxygen mixture at the oxygen content of 40 (1), 20 (2), 10 (3), 5 (4) and 2% (5). *b* — a relevant dependence of specific output  $G_{O_3}$  on the oxygen content.

part of the dependence necessary to calculate the ozone specific output and determine the deviation from linearity. Thus, the total treatment time in all the experiments was 16 min, while the total number of pulses in all the series was 9600. The gas mixture was not discharge-treated during time intervals when the ozone content analysis is performed. The ozone content was determined by the spectrographic method as described in [19] using the Ozone Absorption Table at about 255 nm [20]. The experiments were performed at room temperature, however, the ozone concentration  $[O_3]$  (in ppm) and its specific output ( $G_{O_3}$ ) were in all cases reduced to the normal conditions. Pulse energy  $E_p$  was derived from oscillograms  $U(t)$  and  $I(t)$  for each series via relation  $E_p = \int U(t)I(t)dt$ . Pulse energy  $E_p$  is essentially dependent on the discharge gap parameters and, less essentially, on the composition of the gas mixture under study. For instance, the diagram given in Fig. 1 presents the data on pulse energy  $E_p$  for the studied combinations of the electrode diameter–cylinder diameter parameters. Specific energy  $E$  was calculated for a pulse series via relation  $E = E_p f t / V$ , where  $V$  is the gas mixture volume in the setup ( $V = 26 dm^3$ ). Fig. 2, *a–c* demonstrates the ozone content measurements versus  $E$  for different combinations of the electrode parameters and parameters of pulse energy averaged over the pulse series (see Fig. 1).

Values of the ozone specific output  $G_{O_3}$  were derived from the  $\text{tg } \alpha$  slopes of dependences shown in Fig. 2 by using formula

$$G_{O_3} = \Delta m / (\Delta E V) = M_{O_3} \Delta C / (V_m \Delta E) = M_{O_3} \text{tg } \alpha / V_m, \quad (1)$$

where  $\Delta m$  is the mass of ozone synthesized with introducing energy  $\Delta E$  into the gas mixture unit volume;  $M_{O_3} = 48 g \cdot mol^{-1}$  is the ozone molar mass;  $V_m$  is the gas molar volume under normal conditions ( $V_m = 22.4 dm^3 \cdot mol^{-1}$ );  $\Delta C$  is the ozone concentration increment;  $\text{tg } \alpha = \Delta C / \Delta E$ . Substituting the values and converting the measurement units, obtain a simple formula for calculating  $G_{O_3}$ :

$$G_{O_3} [g \cdot kW \cdot h^{-1}] = 7.714 \text{tg } \alpha [\text{ppm} \cdot dm^3 \cdot J^{-1}]. \quad (2)$$

The specific output values obtained for the dependences shown in Fig. 2 which are approximated by the direct mean square method, are listed in the Table. Notice that the decrease in diameter  $D_e$  from 0.64 to 0.24 mm can hardly affect the discharge parameters (see Fig. 1) and, hence, the ozone generation energy efficiency at different  $D_c$ . An increase in  $D_c$  leads to an increase in  $G_{O_3}$ , however, total amounts of ozone generated during the entire experiment

(9600 discharge pulses) for designs with  $D_c = 90$ , 110 and 145 mm are 34, 27 and 20 mg, respectively, i.e. they decrease with decreasing (as in Fig. 1) pulse energy. Thus, among the studied parameters, values  $D_c = 110$  mm and  $D_e = 0.24$ – $0.64$  mm may be regarded as a compromise variant providing a combination of the setup productivity with high energy efficiency. The found values will be useful in modeling the air purification technologies for assessing energy efficiency of the electrical–to–chemical energy conversion in PCR. To test PCR as an ozone generator, the  $G_{O_3}$  dependence on the oxygen content in the nitrogen–oxygen mixture was studied. Fig. 3, *a* presents the  $E$  dependences of ozone concentration  $[O_3]$  for different oxygen contents, while Fig. 3, *b* demonstrates respective values of  $G_{O_3}$ . In this case, measurements were performed after a series of pulses 2 min long, which may explain an insignificant difference in the slopes of curves presented in Figs. 2, *b* and 3, *a* corresponding to equal discharge chamber parameters and mixture composition  $N_2 : O_2 = 80 : 20$ . Magnitudes of the ozone generation at the oxygen content of 1% have large errors and, thus, are not presented. The obtained dependences need further investigation and simulation of the field strength influence on the ozone production processes.

The proposed method for optimizing the PCR parameters may be used for both designing the ozonators and optimizing PCR parameters in the problems of cleaning air from volatile impurities. Ozone output  $G_{O_3}$  is easily measurable and may be chosen as a criterion for optimizing a specific PCR design and pulse parameters of a high–voltage power–supply generator.

### Financial support

The study was partially supported by the Russian Fundamental Research Foundation and by the Sverdlovsk Region (projects № 20-48-660062 r\_a and 20-08-00882).

### Conflict of interests

The authors declare that they have no conflict of interests.

### References

- [1] S. Jodpimai, S. Boonduang, P. Limsuwan, *J. Electrostat.*, **74**, 108 (2015). DOI: 10.1016/j.elstat.2014.12.003
- [2] Y. Zhu, C. Chen, J. Shi, W. Shangguan, *Chem. Eng. Sci.*, **227**, 115910 (2020). DOI: 10.1016/j.ces.2020.115910
- [3] M. Li, Y. Yan, Q. Jin, M. Liu, B. Zhu, L. Wang, Y.M. Zhu, *Vacuum*, **157**, 249 (2018). DOI: 10.1016/j.vacuum.2018.08.058
- [4] B. Mennad, Z. Harrache, D.A. Aid, A. Belasri, *Curr. Appl. Phys.*, **10** (6), 1391 (2010). DOI: 10.1016/j.cap.2010.04.013
- [5] D. Yuan, Z. Wang, Y. He, S. Xie, F. Lin, Y. Zhu, K. Cen, *Ozone Sci. Eng.*, **40** (6), 494 (2018). DOI: 10.1080/01919512.2018.1476127
- [6] T.L. Sung, S. Teii, C.M. Liu, R.C. Hsiao, P.C. Chen, Y.H. Wu, K. Ebihara, *Vacuum*, **90**, 65 (2013). DOI: 10.1016/j.vacuum.2012.10.003
- [7] B. Liu, J. Ji, B. Zhang, W. Huang, Y. Gan, D.Y. Leung, H. Huang, *J. Hazard. Mater.*, **422**, 126847 (2022). DOI: 10.1016/j.jhazmat.2021.126847
- [8] H. Fukuoka, S. Iida, D. Wang, T. Namihira, in *2019 IEEE Pulsed Power & Plasma Science (PPPS)* (IEEE, 2019), p. 1. DOI: 10.1109/PPPS34859.2019.9009782
- [9] T. Huiskamp, W.F.L.M. Hoeben, F.J.C.M. Beckers, E.J.M. Van Heesch, A.J.M. Pemen, *J. Phys. D: Appl. Phys.*, **50** (40), 405201 (2017). DOI: 10.1088/1361-6463/aa8617
- [10] I.M. Piskarev, *High Energy Chem.*, **54** (3), 205 (2020). DOI: 10.1134/S001814392003011X
- [11] F. Fukawa, N. Shimomura, T. Yano, S. Yamanaka, K. Teranishi, H. Akiyama, *IEEE Trans. Plasma Sci.*, **36** (5), 2592 (2008). DOI: 10.1109/TPS.2008.2004372
- [12] A. Pokryvailo, M. Wolf, Y. Yankelevich, *IEEE Trans. Dielectr. Electr. Insul.*, **14** (4), 846 (2007). DOI: 10.1109/TDEI.2007.4286515
- [13] I.E. Filatov, V.V. Urvarin, E.V. Nikiforova, D.L. Kuznetsov, *J. Phys.: Conf. Ser.*, **2064**, 012094 (2021). DOI: 10.1088/1742-6596/2064/1/012094
- [14] T.I. Poznyak, I.C. Oria, A.S. Poznyak, *Ozonation and biodegradation in environmental engineering* (Elsevier, 2019), p. 325–349. DOI: 10.1016/B978-0-12-812847-3.00021-4
- [15] I. Filatov, V. Uvarin, D. Kuznetsov, in *2020 7th Int. Congress on energy fluxes and radiation effects (EFRE)* (IEEE, 2020), p. 317. DOI: 10.1109/EFRE47760.2020.9242056
- [16] I. Filatov, V. Uvarin, D. Kuznetsov, in *2020 7th Int. Congress on energy fluxes and radiation effects (EFRE)* (IEEE, 2020), p. 322. DOI: 10.1109/EFRE47760.2020.9242070
- [17] S.N. Rukin, *Rev. Sci. Instrum.*, **91** (1), 011501 (2020). DOI: 10.1063/1.5128297
- [18] I.E. Filatov, V.V. Uvarin, D.L. Kuznetsov, *Tech. Phys.*, **63** (5), 680 (2018). DOI: 10.1134/S1063784218050079
- [19] I.E. Filatov, V.V. Uvarin, D.L. Kuznetsov, *Tech. Phys. Lett.*, **46** (1), 94 (2020). DOI: 10.1134/S1063785020010216
- [20] L.T. Molina, *J. Geophys. Res.: Atmospheres*, **91** (D13), 14501 (1986). DOI: 10.1029/JD091iD13p14501